

# Simplicial Diffeomorphisms

Vinícius Mello and Luiz Velho

---

## Abstract

In this paper we will present a theory for simplicial diffeomorphisms, that is, diffeomorphisms that preserve the incidence relations of a simplicial complex. Simplicial diffeomorphisms can be regarded as curvilinear barycentric coordinates. Using the combination of piecewise linear functions on complexes with simplicial diffeomorphisms, we also propose a new representation of curves and surfaces (and hypersurfaces, in general) that is simultaneously implicit and parametric.

*Key words:* Free-form deformations, Barycentric coordinates, Implicit curves and surfaces

---

## 1 Introduction

Spatial transformations are basic operations for geometric modeling, visualization and computer vision. In geometric modeling, deformation techniques such as Free-Form Deformations (FFD) provide powerful tools for shape creation and editing. In visualization, warping and morphing techniques constitute the foundations of most image-based algorithms. In computer vision, projective transformations are at the heart of camera calibration and other fundamental problems.

Implicit surfaces turn out to be particularly suited to deformation based modeling and rendering techniques. In this setting, the surface  $S$  is defined as the inverse image  $f^{-1}(c)$  of a regular value  $c$  of a scalar function  $f : \mathbb{R}^3 \rightarrow \mathbb{R}$  in the ambient space. Therefore, warping the domain of  $f$  causes the surface  $S$  to be deformed.

In order to effectively work with implicit surfaces in the above context, it is necessary to use well behaved spatial transformations. More specifically, the

---

*Email addresses:* `vinicius@mat.ufal.br` (Vinícius Mello), `lvelho@impa.br` (Luiz Velho).

warping must be 1 – 1 and smooth. In other words, a *diffeomorphism*. The main reason for this requirement is that the deformation should preserve the global topology of the level set.

A popular way to create implicit surfaces, and hypersurfaces, in general, is by resorting to a spatial decomposition that allows the construction of the function  $f$  in a piecewise manner. In particular, a simplicial space partition has all the required properties.

The definition of a simplicial implicit hypersurface is as follows: Let  $K$  be a simplicial complex in  $\mathbb{R}^m$  and  $f: V \rightarrow \mathbb{R} - \{0\}$  a function defined on the vertices of  $K$ . It is well known that  $f$  can be extended to a function  $\hat{f}$  defined on the set of points  $|K|$  in  $\mathbb{R}^m$  that belong to the simplexes of  $K$  by linear interpolation. If  $p \in \sigma = \langle v_0, \dots, v_m \rangle$ , do

$$\hat{f}(p) = \sum_{i=0}^m w^i(p) f_{v_i},$$

where  $w^i(p)$  are the barycentric coordinates of  $p$  relative to  $\sigma$ . The implicit hypersurface  $O = \hat{f}^{-1}(c)$  obtained in this way is clearly piecewise linear. Let's call them *linear isocomplexes*.

A linear isocomplex has various important properties that are intimately related with the linear structure of the simplexes which constitute its domain and the piecewise linear function  $\hat{f}$  itself. For example, it is easy to verify if a point  $p \in \mathbb{R}^m$  is inside or outside  $O$ . It is also easy to sample points in  $O$ . On the other hand, if we want to approximate a smooth hypersurface by an isocomplex  $O$ , probably we will have to take a mesh  $K$  with very small simplexes.

To overcome the limitations of the piecewise linear nature of  $\hat{f}$  we can employ a *simplicial diffeomorphism*, that is, a diffeomorphism  $X$  attached to complex  $K$  that preserve its incidence relations. In this way, we are able to produce *curved isocomplexes*  $\mathcal{O} = (\hat{f} \circ X)^{-1}(c)$  while retaining the properties of the simplicial structure. Moreover, simplicial diffeomorphisms incorporate into the implicit hypersurface definition a very powerful deformation based modeling mechanism that can be exploited in many applications.

This paper is organized as follows. In section 2 we relate the concept of simplicial diffeomorphisms to other kinds of generalized barycentric coordinates. In section 3 we present our main theoretical results about simplicial diffeomorphisms. In section 4, we show that simplicial diffeomorphisms combined with isocomplexes provide a new kind of hypersurface representation. Section 5 is devoted to the delicate question of smoothness continuity conditions for curved isocomplexes. We present two applications in section 6 and we finish the paper with a conclusion and discussion of future work in section 7.

## 2 Generalized barycentric coordinates

Barycentric coordinates are ubiquitous in computer graphics and geometric modeling, since they allow to reconstruct continuous data from sampled data. Classically, given a simplex  $\sigma = \langle v_0, \dots, v_m \rangle \subset \mathbb{R}^m$  and a point  $p \in \sigma$ , the barycentric coordinates  $w(p) := (w^0(p), \dots, w^m(p))$  of  $p$  with respect to  $\sigma$  are uniquely defined by the following properties:

$$\text{(partition of unity)} \quad \sum_{i=0}^m w^i(p) = 1 \quad (1)$$

$$\text{(linear precision)} \quad \sum_{i=0}^m w^i(p)v_i = p \quad (2)$$

All other properties of classical barycentric coordinates follow from (1) and (2) above, including:

$$\text{(continuity)} \quad w(p) \text{ is a continuous function of } p \quad (3)$$

$$\text{(interpolation)} \quad w^i(v_j) = \delta_{ij} \quad (4)$$

$$\text{(positivity)} \quad w^i(p) \geq 0 \quad (5)$$

$$\text{(injectivity)} \quad p \neq p' \Rightarrow w(p) \neq w(p') \quad (6)$$

$$\text{(face preservation)} \quad p \in \partial_i \sigma \Rightarrow w^i(p) = 0 \quad (7)$$

where  $\partial_i \sigma$  denotes the face of  $\sigma$  opposite to vertex  $v_i$ . Property (7) says essentially that the interpolation only uses information from the vertices on the same face where  $p$  is, while the meaning of properties (3–6) are obvious.

Being as useful as they are, is natural to seek generalizations of barycentric coordinates. Wachspress extended barycentric coordinates to convex polygons [16, 13]. The Wachspress coordinates satisfies properties (1–5) and recently Floater and Kosinka proved that property (6) also holds [5]. Note that property (7) only makes sense in a simplicial setting. Floater has proposed another kind of generalized barycentric coordinates for convex polygons, the mean value coordinates (MVC) [4]. MVC were further extended to arbitrary polygons [7] and to closed triangular meshes [6, 9]. Ju et al. have treated Wachspress and MVC (and other coordinates) in a unified way [10]. In another direction, Weber et al. have considered complex barycentric coordinates with respect to an arbitrary polygon [17].

In all that cases, the direction of generalizations is from simplicial to polyhedral objects. In this paper, we pursuit another direction: from linear to curvilinear coordinates, in a simplicial context. Specifically, we study what happens when property (2) is dropped, while the others remain. We will see

that it is necessary in order to obtain curved isocomplexes. In a recent paper [8], Huang et al. have considered a kind of curvilinear barycentric coordinates in tetrahedra, though they have not said it explicitly. In their approach, only properties (1), (3) and (4) are ensured.

Suppose that a mapping  $x(p) = (x^0(p), \dots, x^m(p))$  defined on  $\sigma$  satisfies properties (1–7), except property (2). Let's call the numbers  $x^i(p)$  a system of *curvilinear barycentric coordinates*. We have that,

$$\sum_{i=0}^m x^i(p)v_i = q,$$

where  $q$  is different from  $p$ , in general. But from (1) and (3) it follows that  $q$  is a point of  $\sigma$ . Moreover, from (7)  $q$  must be in  $\partial_i\sigma$  whenever  $p$  is. Thus, the mapping  $p \mapsto q$  on  $\sigma$  that results from dropping the linear precision still is face preserving, which bring us the following definiton.

**Definition 1.** Let  $K$  be a simplicial complex and  $X:|K| \rightarrow |K|$  a continuous function. We say that  $X$  is *K-invariant*, if  $X(\sigma) \subset \sigma$  for all  $\sigma \in K$ .

Reciprocally, if  $X$  is a  $\sigma$ -invariant and injective function, we can construct a system of curvilinear coordinates setting

$$x(p) = w(X(p)), \tag{8}$$

where  $w$  are the classical barycentric coordinates. Hence, curvilinear barycentric coordinates and injective  $K$ -invariant functions are essentially two points of view from the same object.

In applications, we need more than just continuity, so let us define the principal concept for now on.

**Definition 2.** Let  $X:|K| \rightarrow |K|$  be a  $K$ -invariant function. We say that  $X$  is a *simplicial diffeomorphism* with respect to complex  $K$  or, more briefly, that  $X$  is a *K-invariant diffeomorphism*, if  $X$  restricted to  $\text{int}(\sigma)$  is a diffeomorphism for all  $\sigma \in K$ , where  $\text{int}(\sigma)$  is the geometric interior of  $\sigma$ .

Note that simplicial diffeomorphisms are not global diffeomorphisms. They are smooth inside each simplex, but not necessarily smooth across faces, just like the classical barycentric coordinates.

### 3 Construction of simplicial diffeomorphisms

In this section we present some constructions of simplicial diffeomorphisms. We focus only in the main results, but a detailed description can be seen in

the technical report [1].

The construction of a simplicial diffeomorphism can be divided in two stages: the first stage consists in to define a  $K$ -invariant mapping  $X$  in a given simplicial complex  $K$ . Initially, we define the functions  $x^i(p)$  in a single simplex  $\sigma$  in such a way that the properties (1), (3–5) and (7) be satisfied, which is generally easy. These functions depend of control parameters associated to faces of  $\sigma$ . To extend the construction to a complex  $K$ , we must ensure that two adjacent simplexes  $\sigma_1$  and  $\sigma_2$  share the same control parameters in its common face  $\delta$ . It is also essential that the coordinates  $x^i(p)$  for  $p \in \delta$  depend only of the control points associated to  $\delta$ . Then, we define  $X$  by equation (8).

The second stage consists precisely in to show that property (6) (injectivity) is satisfied, what is quite difficult in general, because injectivity is a global property. However, applying a classical result from Meisters and Olech [12], we have proved that *a locally injective  $K$ -invariant mapping is necessarily bijective* [1, Corollary 2.7]. Consequently, by the inverse function theorem, if  $X$  is a differentiable  $K$ -invariant mapping with jacobian determinant  $\det(DX) > 0$ , then  $X$  is a simplicial diffeomorphism. That is, the second stage comes to show that a particular function is positive at all points of a simplex  $\sigma$  and for all possible combinations of control parameters associated to  $\sigma$ . Clearly, for this to be possible, it is necessary to impose restrictions to the control parameters.

Next, we describe some types of simplicial diffeomorphisms obtained from this methodology.

### 3.1 Monotonic simplicial diffeomorphisms

Let  $g: [0, 1] \rightarrow [0, 1]$  be a continuous function on the interval  $[0, 1]$  such that  $g(0) = 0$ ,  $g(1) = 1$ . As  $[0, 1]$  is nothing more than a one dimensional simplex, the last condition on  $g$  means only that  $g$  is  $[0, 1]$ -invariant function, in our terminology. It is well known that if  $g'(t) > 0$  for all  $t \in [0, 1]$ , then  $g$  is a diffeomorphism of  $[0, 1]$ , or a simplicial diffeomorphism. Let us generalize that result to higher dimensional simplexes.

Let  $g_i: [0, 1] \rightarrow \mathbb{R}$  be functions such that  $g_i(0) = 0$  and  $g'_i(t) > 0$  for all  $t \in [0, 1]$ , where  $i = 0, \dots, m$ . As the derivative is positive,  $g_i$  is increasing and  $g_i(t) > 0$  if  $t > 0$ . We define the *monotonic barycentric coordinates* in a  $m$ -dimensional simplex  $\sigma$  by

$$x^i(p) = \frac{g_i(w^i(p))}{\sum_{j=0}^m g_j(w^j(p))}. \quad (9)$$

Note the we are just doing a reparametrization of each classical barycentric coordinate, followed by a normalization, in order to achive the partition of

unity property. It is easy to verify the other properties, except the injectivity. But in [1, Section 4], we have proved that such monotonic coordinates are indeed injective.

This result can be extended to a simplicial complex  $K$ , it's enough to define a function  $g_{v_i}$  for each vertex  $v_i$  of  $K$ . Clearly, the monotonic coordinates in a face  $\delta$  shared by two adjacent simplexes  $\sigma_1$  and  $\sigma_2$  only depend of the coordinates associated to the vertices of  $\delta$ .

One feature of this kind of simplicial diffeomorphism, is that all the information about the warping produced by  $X$  is concentrated on vertices, so can be difficult to control what happens in the interior of higher dimensional simplexes.

### 3.2 Polynomial simplicial diffeomorphisms

Generally, a polynomial mapping of degree  $n$   $x: \sigma \rightarrow \mathbb{R}^{m+1}$  can be put in the form

$$x(p) = \sum_{|I|=n} b_I B_I(w(p)), \quad (10)$$

where  $I$  is an integer vector  $(I^0, \dots, I^m)$ ,  $|I| = \sum_i I^i$ ,  $b_I \in \mathbb{R}^{m+1}$  and

$$B_I(W_0, \dots, W_m) = \binom{n}{I^0 \dots I^m} W_0^{I^0} \dots W_m^{I^m}$$

are the *Bézier-Bernstein polynomials* [3]. The points  $b_I$  are called *control points* of  $x$ . In order to  $x$  be a system of curvilinear barycentric coordinates, the points  $b_I$  must satisfy some constraints. For example, the partition of unity property holds if, and only if,  $|b_I| = 1$  for all  $|I| = n$ . Unfortunately, it is difficult to characterize the other properties in terms of conditions on  $b_I$ . Therefore, we content ourselves in to display some sufficient conditions in the control points which ensure all properties.

Let  $\chi$  be a function that associates to each  $m$ -uple  $(p^1, \dots, p^m)$  a  $m$ -uple  $(q^1, \dots, q^m)$  such that

$$q^i = \begin{cases} -1, & \text{if } p^i < 0 \\ 0, & \text{if } p^i = 0 \\ 1, & \text{if } p^i > 0. \end{cases}$$

We say that  $x$  is *adjusted* if  $\chi(b_I) = \chi(I)$  for all  $I$  with  $|I| = n$ . The intuitive idea behind this definition can be resumed as follows: if  $p$  is a point of  $\sigma$ ,  $\chi(w(p))$  is a binary code that identifies the lower dimensional face of  $\sigma$  that contains  $p$ . Thus, setting  $c_I \in \mathbb{R}^m$  as the point such that  $b_I = w(c_I)$ , the

definition means that each point  $c_I$  belongs to face of code  $\chi(I)$ . It is not hard to see that if  $x$  is adjusted, then all properties (3–7) hold, except injectivity. Indeed,  $x$  can be adjusted and not injective if  $x$  has degree greater than 3. It remains to find additional conditions on the control points.

Some sufficient conditions for injectivity are proved in [1, Section 5], for different combinations of degree  $n$  and dimension  $m$ . For instance, we have proved that *if  $x$  is quadratic and adjusted, then  $x$  is injective, for any dimension* [1, Proposition 5.6]. To shorten the presentation, however, we will describe just a set of conditions particularly useful in the applications of section 6.

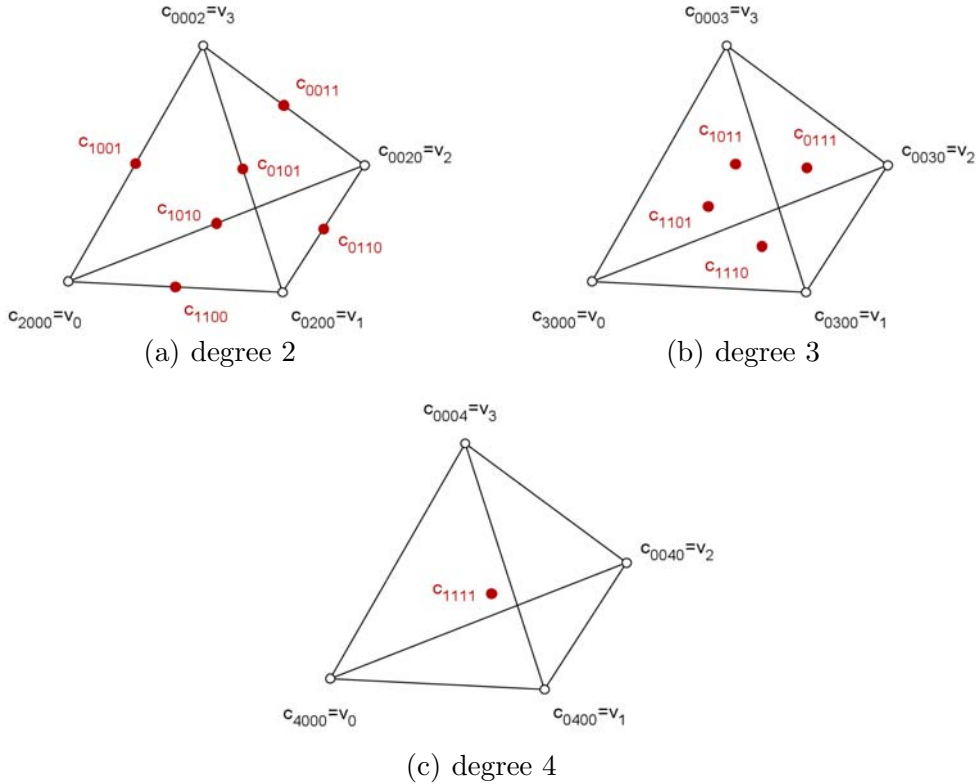


Fig. 1. Adjusted polynomial mappings in a tetrahedron  $\sigma = \langle v_0, v_1, v_2, v_3 \rangle$ : in (a) the solitary points of a quadratic mapping are inside the edges; in (b) the solitary points of a cubic mapping are inside the faces; in (c) the solitary point of a degree 4 mapping is inside the tetrahedron. Every other control points (not showed) are fixed. For any position of the solitary control points, the corresponding mapping is injective.

We say that a control point  $b_I$  is *fixed* if  $b_I = I/n$  and that is *solitary* if  $I^i \in \{0, 1\}$  for all  $i = 0, \dots, m$ . We have proved that *if the non solitary control points of a adjusted polynomial mapping  $x$  are fixed, then  $x$  is injective*. In fact, we proved that only in dimensions 2 and 3 [1, Section 5.3], but we conjecture that it holds for all dimensions. We can see in figure 1 a intuitive idea of the meaning of this proposition.

Hence we have a mapping  $x$  of degree  $n + 1$  that is controlled by the control points located in simplexes of dimension  $n$ , with  $n = 1, 2, 3$ . Each one of such mappings gives rise to a simplicial diffeomorphism  $X_1$ ,  $X_2$  and  $X_3$ , respectively. The compatibility between adjacent tetrahedra is ensured if the control points in each common edge or face are in the same relative position. We call a composition of diffeomorphisms  $X_1$ ,  $X_2$  and  $X_3$ , in some order, a *stratified scheme*. A stratified scheme presents a great power of control, as can be seen in figure 2 and will be demonstrated in more detail in Section 6.

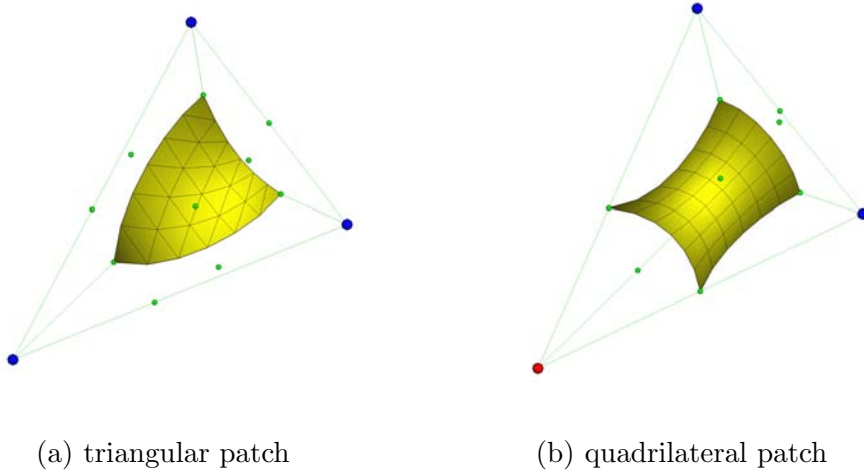


Fig. 2. The result of a composition of diffeomorphisms  $X_1$ ,  $X_2$  and  $X_3$  over a linear patch inside the tetrahedron.

### 3.3 Rational simplicial diffeomorphisms

A rational mapping of degree  $n$   $x: \sigma \rightarrow \mathbb{R}^{m+1}$  can be put in the form

$$x(p) = \frac{1}{\sum_{|I|=n} q_I B_I(w(p))} \sum_{|I|=n} q_I b_I B_I(w(p)), \quad (11)$$

where  $q_I \in \mathbb{R}$  are the *weights* of  $x$ . We define what a adjusted rational mapping is similarly to the polynomial case, and is easy to verify that all properties (3–7) hold, except injectivity.

The analysis of injectivity in the rational case is more difficult, because there is an additional degree of freedom which comes from the weights  $q_I$ . But we have proved that *in an adjusted rational mapping  $x$ , if all the control points are fixed and the weights are positive, then  $x$  is injective, for any dimension* [1, Section 6]. Recently, we learned in [2] that this result follows from Birch’s Theorem, an important theorem in the theory of maximum likelihood estimation for multinomial models. In figure 3 we can see the result of a rational simplicial diffeomorphism.

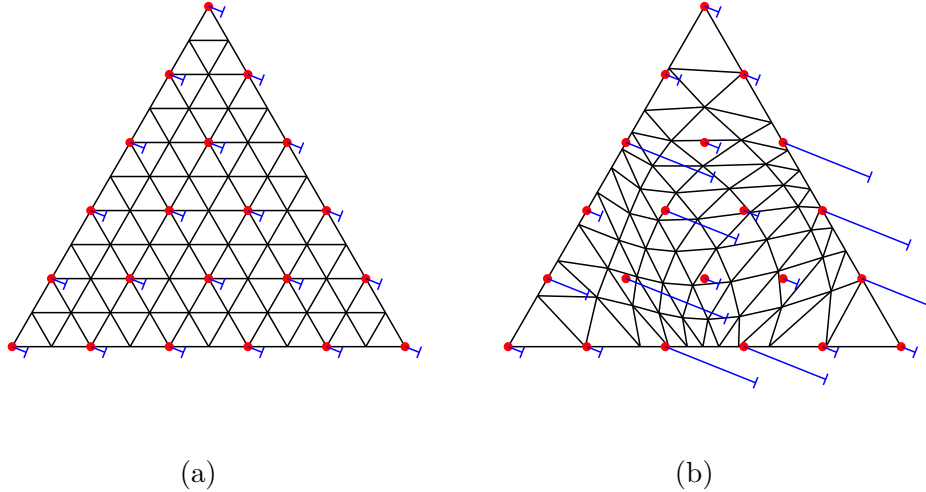


Fig. 3. The action of a rational degree 5 simplicial diffeomorphism: in (a), the control points are fixed and the weights are equal; in (b), some weights were changed. Note that control points with greater weights are more attractive.

#### 4 Curved isocomplexes

In section 1, we define a linear isocomplex as the piecewise linear hypersurface  $\mathcal{O} = \hat{f}^{-1}(c)$ , where  $\hat{f}$  is the piecewise linear function obtained by linear interpolation of a real function  $f$  defined on the vertices of complex  $K$ . If  $X$  is a  $K$ -invariant diffeomorphism, we can use it to deform the set  $|K|$ , obtaining a *curved isocomplex*  $\mathcal{O} = (\hat{f} \circ X)^{-1}(c)$ . As this deformation is bijective, continuous and preserve the incidence relations of  $K$ , it results that  $\mathcal{O}$  has the same topology of  $\mathcal{O}$ . Moreover, the topological and geometrical information of  $\mathcal{O}$  are clearly separated: the topology is codified in the complex  $K$  and in the signal of  $f$  in the vertices, and the geometry is given by  $X$ .

Let's relate this representation with two other representations of hypersurfaces. In the implicit representation, the hypersurface is represented as a zero set of a given equation. In the parametric representation, the hypersurface is represented by a collection of patches that covers the hypersurface and are glued to each other in a precise way. We can write the expression of  $\mathcal{O}$  above in two ways:

$$\mathcal{O} = (\hat{f} \circ X)^{-1}(c) = X^{-1}(\hat{f}^{-1}(c)),$$

The two equalities above have slightly different interpretations. In the first case,

$$\mathcal{O} = (\hat{f} \circ X)^{-1}(c),$$

is clearly a implicit hypersurface, being the set of points  $p \in \mathbb{R}^n$  that satisfies equation  $\hat{f}(X(p)) = c$ . In the second case,

$$\mathcal{O} = X^{-1}(\hat{f}^{-1}(c)),$$

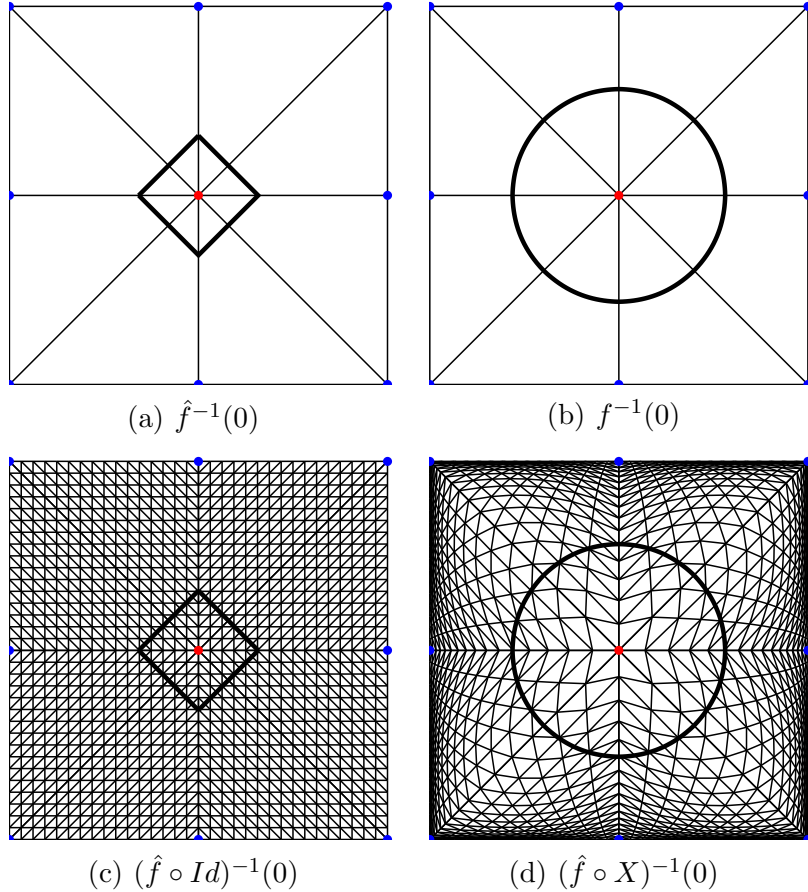


Fig. 4. The zero set of function  $f(x, y) = x^2 + y^2 - 0.28^2$  in four versions: in (a), the linear interpolation over complex  $K$  is far from the real curve (b). Composition with the identity changes nothing (c), but a suitable diffeomorphism  $X$  deforms the linear interpolation closer to the real curve.

says that the set  $\mathcal{O}$  is covered by parametrizations in the form  $X^{-1}(\theta)$ , where  $\theta$  is linear patch of  $\mathcal{O}$ , being therefore a parametric hypersurface. That is why we call this a *implicit-parametric* representation.

Let's consider how the implicit-parametric representation performs in two typical problems: (1) determine if a point  $p \in \mathbb{R}^n$  is inside or outside  $\mathcal{O}$  and (2) sample points  $q \in \mathcal{O}$ . To solve (1), we find which cell  $\sigma \in K$  contains  $p$ , compute  $q = X|_{\sigma}(p)$  and evaluate the signal of  $\hat{f}_{\sigma}(q)$ . For problem (2), we sample a point  $p \in \mathcal{O}$ , what is a easy task because  $\mathcal{O}$  has a simple parametrization for each linear patch  $\theta \subset \sigma \in K$ , and compute  $q = X|_{\sigma}^{-1}(p)$ .

As we have seen, the simplicial diffeomorphism  $X$  depends on a set of *intrinsic parameters*  $\beta$ , therefore we will denote the diffeomorphism by  $X_{\beta}$  when necessary. In the case of polynomial diffeomorphisms, for example,  $\beta$  could be represented by a vector of control points. As we will see in section 6, the main task of the applications is to fit the intrinsic parameters to the data.

## 5 Smoothness conditions for curved isocomplexes

By our definition, a simplicial diffeomorphism  $X$  is a diffeomorphism in the interior of each simplex of  $K$ , but there are no guarantees that  $X$  is a global diffeomorphism and, in fact, in the applications we focus, namely the representation of curved isocomplexes,  $X$  cannot be a global diffeomorphism. Let's understand why this happens.

Let's consider the case of complex  $K = \sigma \cup \sigma'$ , where  $\sigma = \langle p_0, p_1, \dots, p_n \rangle$  and  $\sigma' = \langle p'_0, p_1, \dots, p_n \rangle$ . Note that  $\sigma$  and  $\sigma'$  share a common facet  $\delta = \langle p_1, \dots, p_n \rangle$ . Let  $X$  be a  $K$ -invariant diffeomorphism and  $f$  a real function defined on the vertices of  $K$ . If  $p$  is a point in  $\delta \cap \mathcal{O}$ , the hypersurface normal  $\mathcal{O}$  is proportional to the gradient

$$\nabla(\hat{f} \circ X)(p) = \nabla \hat{f}(X(p)).DX(p).$$

But  $\nabla \hat{f}$  is not well defined in  $\delta$ , because  $\hat{f}$  is only piecewise linear. Let  $n = \nabla \hat{f}|_{\sigma}$  and  $n' = \nabla \hat{f}|_{\sigma'}$ . For  $\mathcal{O}$  to be smooth in  $p$  is necessary that

$$n.DX(p) = n'.DX(p).$$

If  $X$  were smooth at the point  $p$ , then  $DX(p)$  would be not-singular and therefore we would have that  $n = n'$ . In other words,  $\mathcal{O}$  would be smooth in  $\delta$  only if  $\mathcal{O}$  were also smooth. Thus, in order for  $\mathcal{O}$  to be smooth, the simplicial diffeomorphism  $X$  must have a discontinuous derivative in  $\delta$ .

We have to admit that the above fact poses a small difficulty to the analysis, since we are used to continuity conditions and not to discontinuity conditions. Among the various types of simplicial diffeomorphisms that we studied in the previous sections, only in the rational case we were able to derive simple conditions such that  $\mathcal{O}$  be smooth. Suppose that

$$X|_{\sigma}(p) = \frac{1}{\sum_{|I|=n} q_I B_I(w(p))} \sum_{|I|=n} q_I c_I B_I(w(p)) \text{ and,}$$

$$X|_{\sigma'}(p) = \frac{1}{\sum_{|I|=n} q'_I B_I(w'(p))} \sum_{|I|=n} q'_I c'_I B_I(w'(p)),$$

where  $K$  is like described above. Then  $\mathcal{O}$  is  $C^1$ -continuous in  $\delta$  if

$$q_{J+e_0} \hat{f}|_{\sigma}(c_{J+e_0}) = \sum_i w_i q'_{J+e_i} \hat{f}|_{\sigma'}(c'_{J+e_i}), \quad (12)$$

where  $|J| = m - 1$ ,  $J^0 = 0$  and  $(w_0, \dots, w_n)$  are the barycentric coordinates of  $p_0$  in relation to  $\sigma'$  [1, Theorem 8.1].

We can apply the condition (12) to all faces of the complex  $K$ , what originates a system of linear equations in  $q_I$ , in general underdetermined, whose

solutions represent the simplicial diffeomorphisms which make the isocomplex  $O$  smooth. However, we have an additional problem: we are interested in the *positive* solutions, since the weights  $q_I$  should be positive. The investigation of existence conditions of such positive solutions is a very interesting topic which we hope to develop in a future paper. Presently, we can attack this problem using optimization. The idea is to consider the error function

$$\text{err}(\delta, \beta) = \sum_J \|q_{J+e_0} \hat{f}|_{\sigma}(c_{J+e_0}) - \sum_i w_i q'_{J+e_i} \hat{f}|_{\sigma'}(c'_{J+e_i})\|^2,$$

which associates to each face  $\delta$  a value that measures the  $C^1$  discontinuity of the isocomplex in  $\delta$ , where  $\beta$  is a vector containing all the weights  $q_I$ , and then we optimize

$$\min_{\beta > 0} \sum_{\delta \in K} \text{err}(\delta, \beta).$$

We tested this method in an application with very good results, even though some numerical problems might eventually arise due to small values (near zero) in the denominator.

In any case, the smoothness criterion discussed above is valid only for rational mappings. In the case of polynomial mappings, such analysis becomes difficult because the need to reconcile smoothness criteria with injectivity criteria. Furthermore, in the polynomial models that we proposed, we made extensive use of function composition, what makes the analysis even harder. In those cases, the most viable approach is, once again, to deal with the problem through optimization, now considering the error function

$$\text{err}(\delta, \beta) = \sum_{p_i \in \delta} \|n_{\delta, \beta}(p_i) - n'_{\delta, \beta}(p_i)\|^2,$$

which measures the deviation between the normals with respect to the cells  $\sigma$  and  $\sigma'$  incident at a face  $\delta$  in some number of sample points  $p_i$ , where  $\beta$  denote the intrinsic parameters of the diffeomorphism. We have also implemented this other method with good results (see figure 5). Although we cannot guarantee that the surfaces generated in this way will be smooth at all points, we have a more compact representation than a piecewise linear approximation with the added benefits of a simultaneous parametric and implicit representation. As an example, we are going to discuss briefly in the next section some applications of simplicial diffeomorphisms.

## 6 Applications

In this section we are going to present two applications of using the simplicial diffeomorphisms proposed in this paper. These applications are free-form

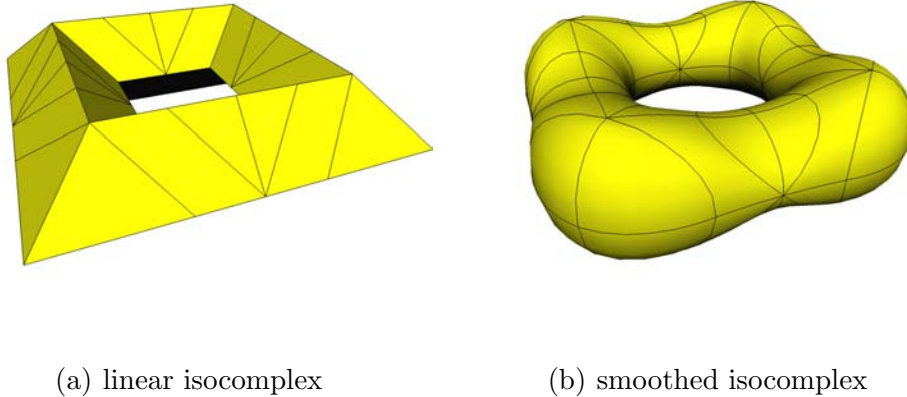


Fig. 5. In (b) we see the result of the smoothing process over the linear isocomplex in (a).

modeling of implicit shapes and adapted polygonization of implicit objects. In both applications, we use the stratified scheme described in section 3.

### 6.1 Free-Form Modeling of Implicit Objects

To present the application of free-form modeling of implicit shapes, first we will briefly describe how the user interacts with the program and subsequently we are going to discuss the implementation.

The basic idea is that the user starts the interaction by visualizing an initial coarse grid  $K_0$ . The user can refine the triangulation using restricted stellar subdivision [11], obtaining a finer simplicial complex  $K$ . At the same time, the user can alter some parameters associated with the vertices and edges of  $K$ , which are going to determine a curved isocomplex  $\mathcal{O}$  with support in  $K$ .

In each vertex  $v$ , the user can make three operations: 1) drag the vertex, moving it to a new position; 2) change the sign  $s(v)$ , making  $v$  to belong either to the interior of the object if  $s(v) = -1$ , or to the exterior of the object if  $s(v) = +1$ ; and change the scalar value  $r(v)$ . These operations allow one to build a linear isocomplex  $\mathcal{O} = \hat{f}^{-1}(0)$ , where  $f(v) = s(v)r(v)$ , which gives a piecewise linear approximation of the object that we wish to model.

In each edge  $\epsilon$  of  $K$  that is intercepted by  $\mathcal{O}$ , the user has access to two controls, which are responsible for controlling the  $K$ -invariant diffeomorphism  $X$ . There is a control handle that can be moved along the edge, indicating the point  $p(\epsilon)$  where  $\mathcal{O}$  should intercept the edge. The other control is a unit

vector  $n(\epsilon)$ , represented by an arrow, that indicates the direction of the normal of  $\mathcal{O}$  should have at  $p(\epsilon)$ , i.e., a *hermite handle*.

These modeling parameters are intuitive for the user, but we need to compute the intrinsic parameters  $\beta$ . For this purpose, we observe that when interpreted mathematically the modeling parameters should satisfy

$$\hat{f} \circ X_\beta(p(\epsilon)) = 0 \text{ and } \frac{\nabla(\hat{f} \circ X_\beta)(p(\epsilon))}{\|\nabla(\hat{f} \circ X_\beta)(p(\epsilon))\|} = n(\epsilon),$$

such that all edges  $\epsilon$  that are intercepted by  $\mathcal{O}$ , that are the ones with vertices with opposite signs. Let's define the error function

$$\text{err}(\sigma, \beta) = \sum_{\substack{\epsilon=\{v_0, v_1\} \in \sigma \\ s(v_0)s(v_1) < 0}} \left( \frac{F_{\sigma, \beta}^2(p(\epsilon))}{\|\nabla F_{\sigma, \beta}(p(\epsilon))\|^2} + \alpha \left\| \frac{\nabla F_{\sigma, \beta}(p(\epsilon))}{\|\nabla F_{\sigma, \beta}(p(\epsilon))\|} - n(\epsilon) \right\|^2 \right),$$

where  $F_{\sigma, \beta} = \hat{f}_\sigma \circ X_\beta$ , that associates to each cell  $\sigma$ , an error  $\text{err}(\sigma, \beta)$  that measures how much the parameters  $\beta$  satisfy the geometric requisites in each cell  $\sigma$ . The parameter  $\alpha$  is a weight that controls how much emphasis is given to the position or direction of the intersection point.

Thus, to determine the parameters  $\beta$ , we simply minimize the error over all cells of  $K$ :

$$\min_{\beta} \sum_{\sigma \in K} \text{err}(\sigma, \beta).$$

Some iterations of this optimization program are performed every time the user updates the modeling parameters. It is possible also to run the optimization program with more interactions in order to obtain a better result. In Figure 6 we show an example of user interaction.

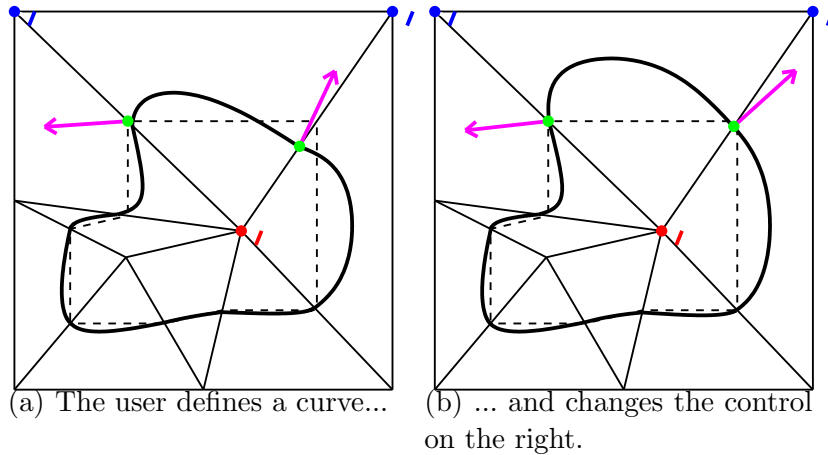
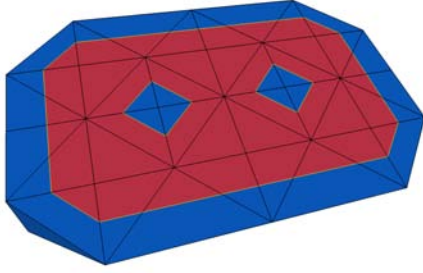
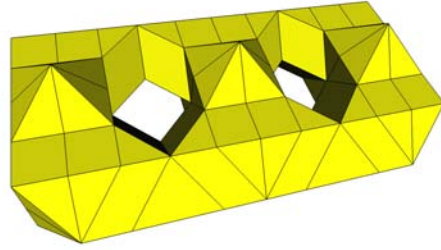


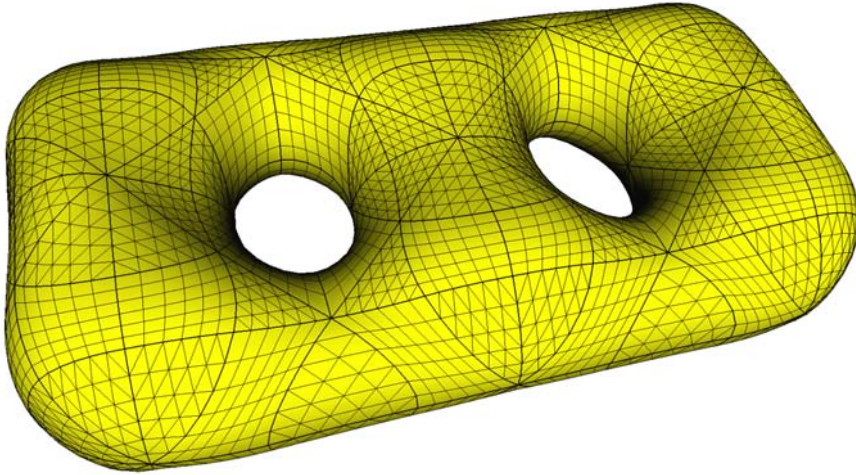
Fig. 6. Example of interaction in the free-form modeling application.



(a) The user defines the interior and exterior points in a tetrahedral mesh



(b) the resulting linear isocomplex



(c) the curved isocomplex, after smoothing

Fig. 7. Example of interaction in the 3-d free-form modeling application. In (c) the triangulation of each patch is shown.

We have implemented a similar application for modeling piecewise implicit surfaces. In Figure 7 we show another example of user interaction in the modeling of a bitorus.

## 6.2 Polygonization of Implicit Objects

The input to the program for polygonization of implicit objects is a function  $g: [0, 1]^n \rightarrow \mathbb{R}$ , which we assume continuous and differentiable. We want to determine a curved isocomplex  $\mathcal{O}$  such that

$$\mathcal{O} \subset g^{-1}((-a, a)),$$

for  $a$  small, in other words, we would like that  $\mathcal{O}$  lies on a neighborhood of  $g^{-1}(0)$ .

The idea is to build a sequence of isocomplexes  $\mathcal{O}_i = (\hat{f}_i \circ X_{\beta_i})^{-1}(0)$  that approximates  $g^{-1}(0)$ . We set initially  $K_0$  equal to the canonical triangulation of  $[0, 1]^n$ ,  $f_0(v) = g(v)$ , for all  $v \in K_0$ , and  $X_{\beta_0}$  equal to identity. In order to describe the inductive step that computes  $\mathcal{O}_{i+1}$  from  $\mathcal{O}_i$ , we need to define a function  $\text{err}(\sigma_i, \beta_i)$  which associates to each cell  $\sigma_i \in K_i$  an error that measures how close  $\mathcal{O}$ , restricted to  $\sigma_i$ , is from  $g^{-1}(0)$ .

Let  $\theta_i$  be the linear patch of  $\mathcal{O}$  in  $\sigma_i$ . We compute the  $m$  sample points  $p_1, \dots, p_m$  over  $\theta_i$  and define

$$\text{err}(\sigma_i, \beta_i) = \sum_{p_j \in \theta_i} |g(X_{\beta_i}(p_j))|^2,$$

that is,  $\text{err}(\sigma_i, \beta_i)$  measures how well  $\theta_i$  is taken to  $g^{-1}(0)$  by  $X_{\beta_i}$ .

The inductive step is done in the following way: we choose the cell  $\sigma_i \in K_i$  with the largest error. Subsequently we perform

$$K_{i+1} = \text{SUBDIVIDE}(K_i, \sigma_i),$$

where  $\text{SUBDIVIDE}(K, \sigma)$  represents the subdivision of  $\sigma$  with adaptive propagation [15].

After such subdivision,  $k$  new vertices  $v_1, \dots, v_k$  are inserted, in that order. For each vertex  $v_k$ , we make  $f_{i+1}(v_k) = g(v_k)$ ,  $f_{i+1}$  being equal to  $f_i$  in the other vertices, and we execute the optimization program.

$$\min_{\beta_{i+1}} \sum_{\sigma_{i+1} \in \text{st}(v_k, K_{i+1})} \text{err}(\sigma_{i+1}, \beta_{i+1}),$$

in order to compute  $X_{\beta_{i+1}}$ . Notice that in this way we are computing  $X_{\beta_{i+1}}$  only in the regions of the mesh that were modified by the subdivision.

The stopping criterion is based on the one described in [14]. Let  $I_\sigma$  be the smallest  $n$ -dimensional box which contains a cell  $\sigma$ . The inclusion function  $\square g$  for a function  $g$  computes for each  $n$ -dimensional box  $I_\sigma$  an interval  $\square g(I_\sigma)$  such that

$$x \in I_\sigma \Rightarrow g(x) \in \square g(I_\sigma).$$

Such an inclusion function for  $g$  can be computed by the usual methods of interval or affine arithmetic. Before evaluating the subdivision in a cell  $\sigma$ , we evaluate the condition

$$0 \notin \square g(I_\sigma) \vee \langle \square \nabla g(I_\sigma), \square \nabla g(I_\sigma) \rangle > 0.$$

If the condition is true, the subdivision is not done, that is, if  $\sigma$  does not contain a zero of  $g$  or if  $g$  is parametrizable along one direction, then it is not necessary to perform the subdivision.

In Figures 8, 9 and 10 we show the polygonization algorithm applied to Taubin's curve,

$$0.004 + 0.110x - 0.177y - 0.174x^2 + 0.224xy - 0.303y^2 -$$

$$0.168x^3 + 0.327x^2y - 0.087xy^2 - 0.013y^3 +$$

$$0.235x^4 - 0.667x^3y + 0.745x^2y^2 - 0.029xy^3 + 0.072y^4 = 0,$$

in three distinct stages. Note how the geometry is well captured, even with a small number of subdivisions.

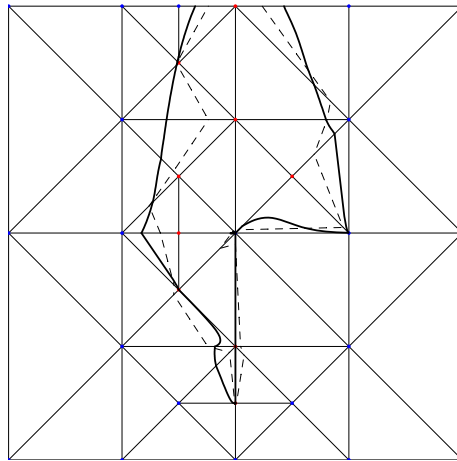


Fig. 8. Polygonization of Taubin's curve (1).

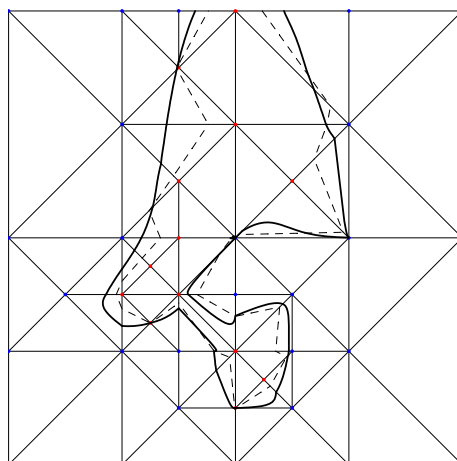


Fig. 9. Polygonization of Taubin's curve (2).

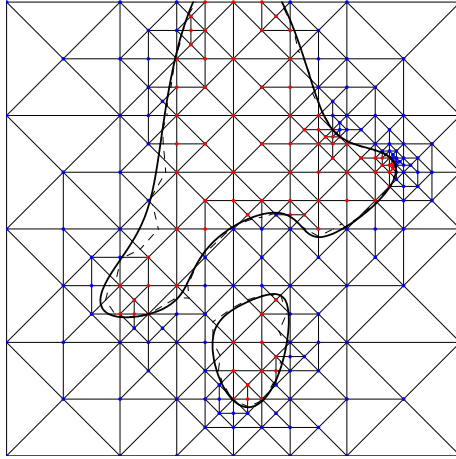


Fig. 10. Polygonization of Taubin's curve (3).

## 7 Conclusion

We have presented a theory of simplicial diffeomorphisms. This type of spatial mapping is very powerful and can be used in several applications. In particular, it can be applied to the piecewise description of shapes through curved isocomplexes. Simplicial diffeomorphisms can also be employed as a general warping mechanism with intuitive controls.

We have shown how to define simplicial diffeomorphisms using the notion of simplicial invariant functions and three alternative ways to construct them with different properties: using monotonic functions; using polynomial basis; and rational polynomials.

We have also discussed conditions to enforce smoothness for curved isocomplexes generated with simplicial diffeomorphism, and demonstrated examples of applications to free-form modeling and implicit surface approximation.

As we just started the study of modeling based on simplicial diffeomorphisms, we believe that there is considerable room for improvements. For instance, for this representation to be competitive with other representations, it is necessary to have in one hand the least possible amount of tetrahedra. In the other hand, this increases the number of control parameters necessary to model the surface patch inside each tetrahedron. To find the proper balance, we must consider new tetrahedralization methods and new kinds of simplicial diffeomorphisms. In any case, we believe that modeling based on simplicial diffeomorphisms can be useful in applications like collision detection, where the implicit-parametric duality of this representation can be better exploited.

## References

- [1] Vinícius Mello and Luiz Velho. Simplicial diffeomorphisms. Technical Report A-632, IMPA, 2009. URL [http://www.preprint.impa.br/Shadows/SERIE\\_A/2009/632.html](http://www.preprint.impa.br/Shadows/SERIE_A/2009/632.html).
- [2] G. Craciun, L.D. García-Puente, and F. Sottile. Some geometrical aspects of control points for toric patches. In *Mathematical Methods for Curves and Surfaces*, pages 111–135. Springer Berlin/Heidelberg, 2010.
- [3] G. Farin. Triangular Bernstein-Bézier patches. *Computer Aided Geometric Design*, 3(2):83–127, 1986.
- [4] Michael S. Floater. Mean value coordinates. *Comput. Aided Geom. Des.*, 20(1):19–27, 2003.
- [5] Michael S. Floater and Jiří Kosinka. On the injectivity of wachspress and mean value mappings between convex polygons. *Advances in Computational Mathematics*, to appear, 2009.
- [6] Michael S. Floater, Géza Kós, and Martin Reimers. Mean value coordinates in 3d. *Comput. Aided Geom. Des.*, 22(7):623–631, 2005.
- [7] Kai Hormann and Michael S. Floater. Mean value coordinates for arbitrary planar polygons. *ACM Trans. Graph.*, 25(4):1424–1441, 2006.
- [8] Jin Huang, Lu Chen, Xinguo Liu, and Hujun Bao. Efficient mesh deformation using tetrahedron control mesh. *Comput. Aided Geom. Des.*, 26(6):617–626, 2009.
- [9] Tao Ju, Scott Schaefer, and Joe Warren. Mean value coordinates for closed triangular meshes. *ACM Trans. Graph.*, 24(3):561–566, 2005.
- [10] Tao Ju, Peter Liepa, and Joe Warren. A general geometric construction of coordinates in a convex simplicial polytope. *Comput. Aided Geom. Des.*, 24(3):161–178, 2007.
- [11] Esdras Medeiros, Helio Lopes, Thomas Lewiner, Geovan Tavares, and Luiz Velho. Topological mesh operators. *Computer Aided Geometric Design*, 2009.
- [12] G. Meisters and C. Olech. Locally one-to-one mappings and a classical theorem on schlicht functions. *Duke Mathematical Journal*, 30:63–80, 1963.
- [13] Mark Meyer, Alan Barr, Haeyoung Lee, and Mathieu Desbrun. Generalized barycentric coordinates on irregular polygons. *J. Graph. Tools*, 7(1):13–22, 2002.
- [14] S. Plantinga and G. Vegter. Isotopic approximation of implicit curves and surfaces. In *Eurographics Symposium on Geometry Processing*, pages 245–254. The Eurographics Association, 2004.
- [15] Luiz Velho. A dynamic adaptive mesh library based on stellar operators. *Journal of Graphics Tools*, 9(2):1–29, 2004.
- [16] E. Wachspress. *A Rational Finite Element Basis*. Academic Press, 1975.
- [17] Ofir Weber, Mirela Ben-Chen, and Graig Gotsman. Complex barycentric coordinates with applications to planar shape deformation. *Computer Graphics Forum*, 28(2):587–597, 2009.